Complexity in a Simple Self-Assembling System: Lecithin-Water-Ethanol Mixtures Exhibit a Re-Entrant Phase Transition and a Vesicle-Micelle Transition (VMT) on Heating

Faraz A. Burni, Niti R. Agrawal, Maxwell Walker, Hamna Ali, and Srinivasa R. Raghavan*

Department of Chemical & Biomolecular Engineering, University of Maryland, College Park, Maryland 20742, USA †Equal contribution.

Abstract: We report surprising results for the self-assembly of lecithin (a common phospholipid) in water-ethanol mixtures. Lecithin forms vesicles (~ 100 nm diameter) in water. These vesicles are transformed into small micelles (~ 5 nm diameter) by a variety of destabilizing agents such as single-tailed surfactants and alcohols. In a surfactant-induced vesicle-micelle transition (VMT), vesicles steadily convert to micelles upon adding the surfactant—thereby, the turbidity of the solution drops monotonically. Instead, when an alcohol like ethanol is added to lecithin vesicles, we find a new, distinctive pattern in phase behavior as the ethanol fraction f_{eth} in water is increased. The turbidity first decreases (from $f_{\text{eth}} = 0$ to 37%), then rises sharply ($f_{\text{eth}} = 37$ to 50%), and then eventually decreases again ($f_{\text{eth}} > 55\%$). Concomitant with the turbidity rise, the vesicles separate into two phases around $f_{\text{eth}} = 50\%$ before a single phase reappears at higher f_{eth} — in other words, there is a 're-entrant' phase transition from 1-phase to 2-phase and back to 1-phase with increasing f_{eth} . Vesicles near the phase boundary ($\sim f_{\text{eth}} = 45\%$) also show a VMT upon heating. Similar patterns are seen with other alcohols such as methanol and propanol. We ascribe these complex trends to the dual role played by alcohols: (a) firstly, alcohols reduce the propensity for flat lipid bilayers to bend and form closed spherical vesicles; and (b) secondly, alcohols diminish the tendency of lipids to self-assemble in the solvent mixture. At low alcohol fractions, (a) dominates, causing the initially unilamellar vesicles to grow into multilamellar vesicles (MLVs), which eventually phase-separate. Thereafter, (b) dominates, and the vesicles convert into micelles. Support for our hypothesis comes from scattering (SANS) and microscopy (cryo-TEM). Thus, we have uncovered a general paradigm for lipid self-assembly in solvent mixtures, and this may even have physiological relevan

Keywords: Lipid phase behavior, liposomes, ethosomes, thermoresponsive vesicles, smart vesicles, turbidimetry.

Introduction

The spontaneous organization of amphiphilic molecules in water by self-assembly is a hallmark of biology. $^{1-5}$ The typical amphiphiles in mammalian cells are *phospholipids*, which are generically termed 'lecithins'. 6 These lipids have a phosphatidylcholine head that is hydrophilic and two alkyl tails that are hydrophobic. When lecithin is added to water, it assembles into bilayer membranes (so-called because the lipids are arranged in a head-tail-tail-head fashion). 4,5 These membranes, in turn, can fold to form closed spherical structures, i.e., vesicles (Figure 1): note that the vesicle diameter is typically ~ 100 nm while the bilayer thickness is ~ 5 nm. Lecithin vesicles are a major component of bile, the fluid secreted by the liver that is important for digestion. 7,8

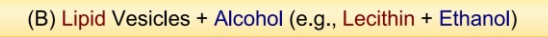
One focus of this paper is on the spontaneous transformation of vesicles to micelles. In a micelle, the tails of the amphiphiles are directed towards the core while the heads are on the periphery; thus, micelles have a hydrophobic (oily) core whereas vesicles have an aqueous core. 4,5 Spherical micelles, with diameters ~ 5 nm, are also much smaller than vesicles. Accordingly, a sample containing micelles will appear clear whereas a vesicle suspension will appear turbid due to light-scattering from the larger vesicles. 9 Vesicle-micelle transitions (VMTs) can be induced by several routes. For example, if lecithin vesicles are combined with a single-tailed nonionic surfactant like Tween 80 or Triton X-100¹⁰⁻¹³ or a bile salt like sodium cholate or sodium dexoycholate, 14-17 a VMT will occur, i.e., the vesicles will get 'solubilized' to form spherical micelles. In a physiological context, a VMT is expected to continuously arise in bile (a fluid that contains both lecithin and bile salts) as it is transported from the bile duct from the liver to the gall bladder.^{7,18}

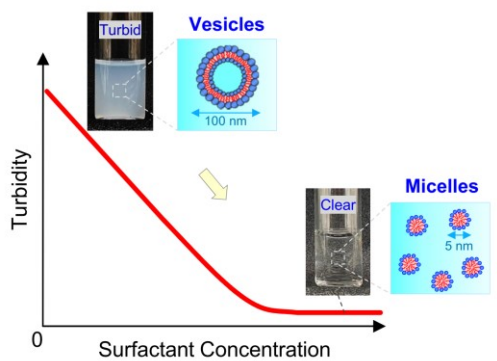
Over the past decades, the science of self-assembly has been elaborated in textbooks.²⁻⁵ VMTs can now be broadly understood in geometric terms: specifically, in terms of the critical packing parameter CPP = a_{tail} / a_{head} . The CPP is the ratio of cross-sectional areas of the tail (a_{tail}) and head (a_{head}) regions of the amphiphile.^{4,5} Lipids have a CPP ~ 1, i.e., their head and tail areas are nearly equal (due to their two tails), which explains why they form vesicles.⁵ Surfactants with a single tail have a CPP much less than 1, which is conducive to forming micelles instead.⁵ Thus, adding a surfactant to lipid vesicles reduces the net CPP and thereby drives a VMT. 10 Such a VMT can be easily detected by measuring the turbidity of the sample. 12,15 For example, we show a schematic plot of the turbidity in Figure 1A for lipid (e.g., lecithin) vesicles upon adding a surfactant (e.g., Tween 80) (see Figure S1 for actual data). As the surfactant concentration is increased, the sample steadily transforms from a turbid state, indicative of vesicles, to a clear state (turbidity ~ 0), indicative of micelles. 12,15 Thus, a surfactant-induced VMT occurs in a predictable manner.

Vesicles can also be transformed to micelles by adding alcohols, a simple example being ethanol. ¹⁹ Consider the system of lipid vesicles (e.g., lecithin) in water + ethanol, which is the focus of this paper. On first glance, one might expect this simple system to behave in a similar manner to the lipid-surfactant mixtures in Figure 1A. Indeed, ethanol does induce a VMT when its content is high. However, the striking findings from our study are that this system is much more complicated. The differences are shown by a schematic plot of the turbidity vs. ethanol fraction $f_{\rm eth}$ (Figure 1B) (see Figure 2 below for actual data).

^{*}Corresponding author. Email: sraghava@umd.edu







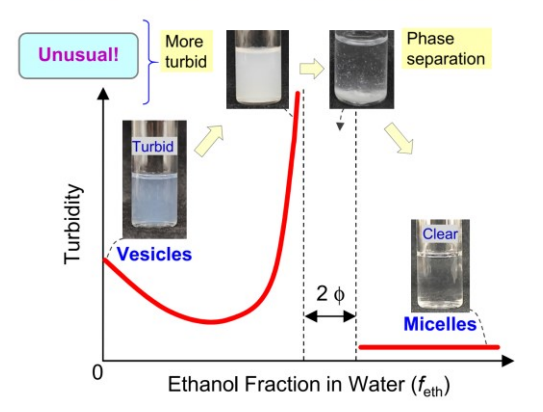


Figure 1. How lipid vesicles are affected by surfactants vs. alcohols. The effects are shown by schematic plots of the turbidity vs. additive concentration. (A) When a surfactant is added, the turbid sample steadily becomes clear, as the vesicles (~ 100 nm) transform into micelles (~ 5 nm). (B) When an alcohol is added, the turbidity first decreases, then increases sharply, followed by a 2-phase (2 ϕ) region, and then a clear state (data in Figure 2). The vesicles do finally become micelles, as in (A), but the intermediate states are unusual. These findings are discussed and explained in this paper.

As $f_{\rm eth}$ is increased, the turbidity first decreases, then rises sharply, and then eventually decreases again to near-zero. In conjunction with the turbidity rise, the vesicles separate into two phases around $f_{\rm eth} = 50\%$ before a single phase emerges again at higher $f_{\rm eth}$. Also, vesicles near the phase boundary ($\sim f_{\rm eth} = 40\%$) show a VMT upon heating. To our knowledge, these results have not been reported in the literature. In fact, although lecithin-water-ethanol mixtures have been studied for more than 50 years, 20 no detailed studies on their phase behavior have yet been published. Here, we report a comprehensive study using a variety of techniques, including UV-Vis spectroscopy, dynamic light scattering (DLS), nanoparticle tracking analysis (NTA), small-angle neutron scattering (SANS), and cryo-transmission electron microscopy (cryo-TEM).

What causes the complex phase behavior of lecithin-water-ethanol mixtures? We will provide a physical explanation for these results based on the fundamentals of lipid self-assembly. ²⁻⁵ Briefly, ethanol plays a dual role: (a) on the one hand, it reduces the propensity for flat lipid bilayers to bend and form closed spherical vesicles; and (b) on the other hand, it diminishes the tendency of lipids to self-assemble in the solvent mixture. Around $f_{\text{eth}} = 50\%$, (a) dominates, and therefore, the initially unilamellar vesicles grow into multilamellar vesicles (MLVs), which eventually phase-separate. At higher f_{eth} , (b) dominates, inducing the vesicles to transform into micelles. If ethanol is substituted by other alcohols such as methanol or propanol, the same trends in phase behavior arise. Thus, we have uncovered a general paradigm for lipid self-assembly in solvent mixtures.

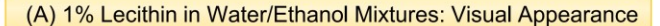
The significance of our study may extend beyond mere scientific curiosity. As noted earlier, VMTs occur in the bile duct and hence have physiological relevance. It is well-known that over-consumption of alcohol affects the liver — these deleterious effects may well be linked to how alcohol affects lipids and alters the above VMT. ²¹⁻²³ Vesicles of lecithin in water-ethanol mixtures may also be useful in delivery applications. ^{24,25} In particular, vesicles that penetrate skin are greatly desired for the transdermal delivery of drugs, vaccines, and cosmetics. ²⁴ While conventional lipid vesicles do not penetrate skin,

it has been shown that vesicles of lipids (like lecithin) combined with ethanol can indeed penetrate through the stratum corneum into the viable epidermis (such vesicles have been termed transfersomes or ethosomes). ^{24,25} We postulated in an earlier study that the coexistence of vesicles and micelles in such samples may be the key to their skin-penetrating ability. ²⁶ Thus, our findings from the present study may also guide the design of vesicle formulations for delivery applications. In that regard, note also that a VMT will involve release of the payload encapsulated in the aqueous core of the vesicles. Hence, a VMT upon heating could also be useful in the context of drug delivery. ²⁷⁻³⁰

Results and Discussion

Lecithin in Water-Ethanol Mixtures. Figure 2 presents the effect of ethanol on lecithin vesicles in water. The lecithin we have used is soy phosphatidylcholine, which has been studied extensively. 13 We fix the lecithin concentration and vary the ethanol fraction f_{eth} from 0 to 60%. Photos of sample vials are shown in Figure 2A for 1 wt% lecithin. The turbidity of the samples is quantified using UV-vis spectroscopy and plotted as the optical density (OD) at a wavelength of 500 nm in Figure 2B. These data are for 0.5% lecithin to make sure the OD values fall within the measurement scale. Both the photos and the turbidity data reveal the same trends. First, note that vesicle samples are expected to be turbid due to light scattering from vesicles ~ 100 nm diameter. When water is replaced with low amounts of ethanol, i.e., for feth from 0 to about 37%, the turbidity drops. The samples thereby turn from a milky white color to a pleasing bluish tinge. Next, when feth is increased from 37% to 45%, the turbidity rises sharply. Figure S2 shows a close-up of the data with additional data points near the minimum at 37%.

As f_{eth} is increased beyond 45%, the samples separate into two phases. Samples in the 46% to 54% range initially appear white and opaque soon after preparation, as can be noted from the vial for 50% f_{eth} in Figure 2A. But after a day, a sample that was homogeneous and white develops a clear phase boundary: a white precipitate appears at



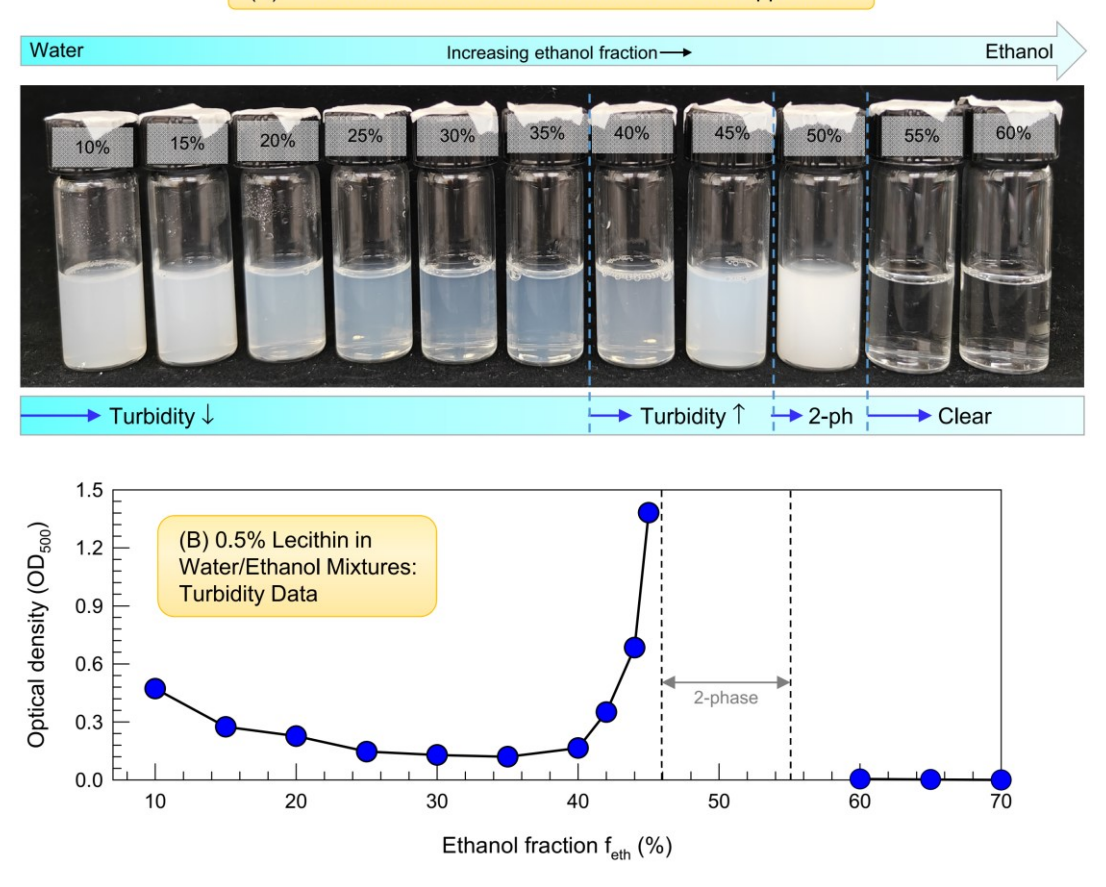


Figure 2. Self-assembly of lecithin in water-ethanol mixtures. (A) Vial photos for 1% lecithin with varying ethanol. (B) Plot of the optical density at 500 nm (OD $_{500}$) (a measure of turbidity) for 0.5% lecithin vs. the ethanol fraction f_{eth} in the solvent. The photos track the turbidity changes in the plot: a decrease, then a sharp rise up to a 2-phase region, and then a clear region. The 2-phase sample at 50% ethanol is highly turbid in the photo, but over time, it separates into two distinct phases: a clear supernatant and a precipitate (see Figure S3).

the bottom of the vial along with a clear supernatant (see photos in Figure S3). Finally, when $f_{\rm eth}$ is increased to 55% or more, the samples become clear (turbidity ~0) and one phase. Similar trends are observed at other lecithin concentrations as well. Data for 0.1% and 0.3% lecithin (Figure S4) closely resemble the curve for 0.5% lecithin in Figure 2B. Thus, we conclude that the lecithin-water-ethanol system shows a *re-entrant phase transition*, 31,32 where upon changing a compositional variable (ethanol content in this case), the system transforms from 1-phase to 2-phase and then eventually reverts back to 1-phase.

To probe this system further, we first turned to dynamic light scattering (DLS). The hydrodynamic diameter (D_h) measured by DLS is shown in Figure 3 for samples with 0.5% lecithin at various $f_{\rm eth}$. Note that, for the D_h calculation, we used the correct viscosity of the solvent (i.e., the water/ethanol mixture) in each sample. This viscosity is needed in the Stokes-Einstein equation to convert the diffusivity measured by DLS to a value of D_h . 4.5 The D_h for lecithin vesicles starts at about 60 nm for $f_{\rm eth} = 0$ to 10%. As $f_{\rm eth}$ is increased from 10% to 37%, D_h steadily increases to about 120 nm. The increase in vesicle size over this range of $f_{\rm eth}$ occurs despite the samples showing a drop in turbidity (Figure 2B).

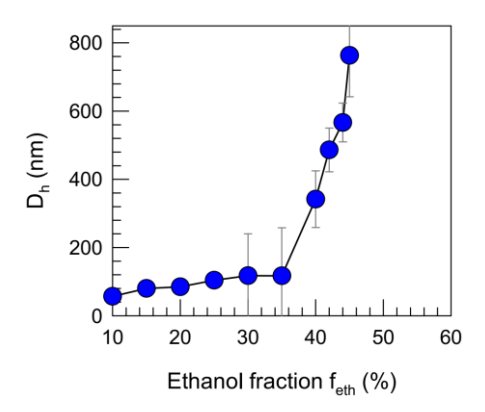


Figure 3. Sizes of lecithin vesicles in water-ethanol mixtures. Samples containing 0.5% lecithin are studied by DLS and the hydrodynamic diameter ($D_{\rm h}$) is plotted vs. $f_{\rm eth}$. The values shown are means and the error bars represent standard deviations.

Note also the large error bars for D_h in the 30-37% range. For these samples, when the DLS data are analyzed as particle size distributions (PSDs), two distinct peaks are seen in the PSDs. This is revealed by Figure S5: the $f_{\rm eth} = 35\%$ has two peaks in its PSD (Figure S5B), whereas only one narrow peak is seen in the PSD for $f_{\rm eth} = 10\%$ (Figure S5A). The bimodal PSD is the reason for the large standard deviations

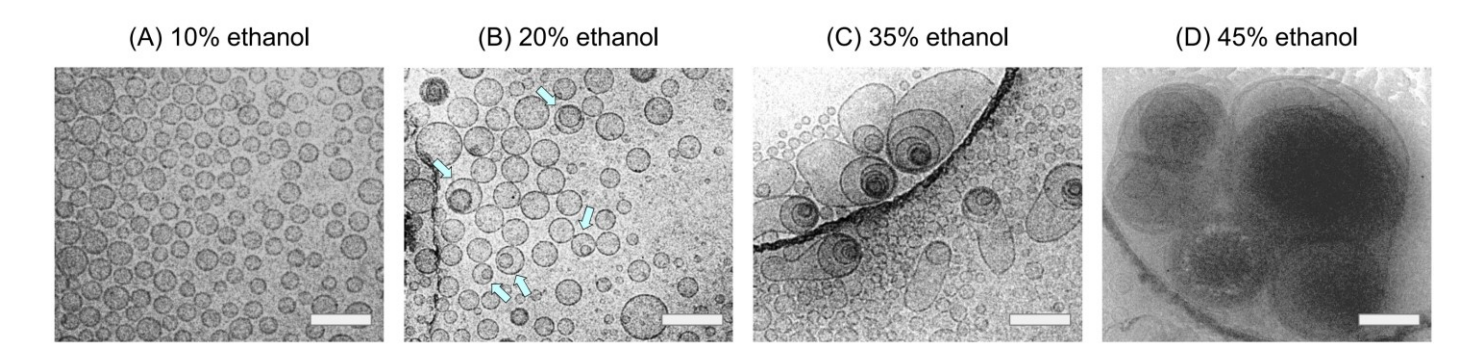


Figure 4. Cryo-TEM images of lecithin vesicles in water-ethanol mixtures. A transition from unilamellar vesicles (ULVs) to multilamellar vesicles (MLVs) is seen as the ethanol fraction is increased. (A) has only ULVs; (B) has mostly ULVs and a few vesicles with two lamellae (arrows); (C) has large MLVs coexisting with small ULVs; and (D) has very large MLVs. Scale bars: 200 nm.

in the average diameter for $f_{\text{cth}} = 35\%$. We further infer that this sample must contain two populations of vesicles, one larger and one smaller.

Above $f_{\rm eth} = 37\%$, a sharp increase in $D_{\rm h}$ is seen in Figure 3. $D_{\rm h}$ is about 350 nm for $f_{\rm eth} = 40\%$ and increases to about 800 nm for $f_{\rm eth} = 45\%$. Such large diameters are indicative of multilamellar vesicles (MLVs), i.e., vesicles with many concentric bilayers. ^{5,9} In contrast, the smaller vesicles at low $f_{\rm eth}$ are expected to be unilamellar vesicles (ULVs). Thus, from DLS, we infer that ethanol induces a transition of lecithin vesicles from ULVs to MLVs. The MLVs grow until the phase boundary is reached at $f_{\rm eth} = 46\%$. After the 2-phase region (46% to 54%), the clear samples at $f_{\rm eth} = 55\%$ and higher can also be analyzed and are found to have small nanostructures ($D_{\rm h} < 20$ nm) in them. These sizes are consistent with spherical or ellipsoidal micelles. Thus, when sufficient ethanol is added to lecithin vesicles, we do observe a vesicle-micelle transition (VMT).

How can we understand the drop in turbidity from $f_{\text{eth}} = 10$ to 37% that accompanies the increase in vesicle size over this range of ethanol concentrations? Generally, a drop in turbidity can signify a decrease in either the size or concentration of the vesicles. Here, we have ruled out the former — hence, there must be a change in the vesicle concentration, i.e., a transition to fewer, but larger vesicles. To confirm this point, we turned to a relatively new technique called nanoparticle tracking analysis (NTA).33 This technique, which utilizes Miescattering theory, allows us to measure the number density of nanoparticles in a given sample. Data from NTA for samples with 0.5% lecithin at various f_{eth} (10 to 35%) are shown in Figure S6. At higher f_{eth} the data were noisy and are hence not shown. But we do see the expected trend for the number density (N_{ves}) over the range shown: it decreases from 4×10^{12} vesicles/mL for $f_{\text{eth}} = 10\%$ to 1.5×10^{11} vesicles/mL for $f_{\text{eth}} = 35\%$. Over the same range of f_{eth} the vesicle diameter (Dh) increases from 60 to 120 nm. Thus, the number of vesicles decreases 20-fold while the size increases 2-fold. All in all, the data from turbidity, DLS, and NTA together confirm an ethanolinduced transition from numerous small vesicles to fewer large vesicles.

Support for the above nanostructural transition comes from cryo-TEM. In this technique, aqueous samples are rapidly cooled so as to vitrify the water in them and thereby preserve the nanostructures present. ¹³ Representative cryo-TEM images are shown in Figure 4 for 0.5% lecithin in various $f_{\rm eth}$. At $f_{\rm eth} = 10\%$ (Figure 4A), the sample

contains numerous small vesicles (ULVs) with diameters < 100 nm, consistent with the DLS data. When feth is increased to 20% (Figure 4B), we see mostly ULVs in the sample and these are about the same size as those in Figure 4A. There are also several vesicles with two concentric bilayers, which are marked with arrows. Next, at $f_{\text{eth}} = 35\%$ (Figure 4C), the nanostructure is quite different. We find both small ULVs and much larger MLVs, consistent with the bimodal size distribution from DLS. The MLVs have 3-5 concentric bilayers and their sizes are > 300 nm. Some vesicles look elongated, but this may be an artifact caused by the shear exerted on a sample in the blotting step during cryo-TEM grid preparation (see Experimental Section). Finally, at $f_{\text{eth}} = 45\%$ only a few large MLVs are seen in the sample. These vesicles appear dark, likely because each of them has numerous closely-spaced bilayers (the dark color in TEM images arises when the electron beam gets scattered through large, dense structures). Together, the images in Figure 4 again show the transition from small ULVs to large MLVs as f_{eth} is increased.

Additional support comes from SANS. We performed SANS experiments on 0.5% lecithin vesicles in deuterated water-ethanol mixtures. Figure 5 shows plots of the scattering intensity I vs. wave vector q plots for various f_{eth} . Because lecithin is a zwitterionic lipid and there are no other charged molecules in the samples, the data in Figure 5 mainly reflects the shapes of the scatterers in each sample. That is, I(q) is dictated simply by the form factor P(q).³⁴ Typically, vesicle samples exhibit a slope of -2 in SANS spectra at low to intermediate q — this slope is indicative of the P(q) corresponding to flat sheets, which corresponds to the lamellar bilayers surrounding the vesicle cores (i.e., $I \sim q^{-2}$).^{29,34} Indeed, a slope close to -2 is seen for samples with $f_{\text{eth}} = 15\%$ and 30% (Figures 5A and 5B).

Next, regarding the sample with 50% ethanol (Figure 5C), it is highly turbid initially (see inset photo) and thereafter separates into two phases over a day. It was studied by SANS right after preparation. The SANS data show a slope of -4, reflecting Porod's law ($I \sim q^{-4}$) for scattering from interfaces.³⁴ Such interfaces can arise as the sample phase-separates — thus, SANS is able to pick up the initial stages of this phase separation. The sample also shows a Bragg peak at $q^* = 0.12$ Å⁻¹. The length scale d corresponding to this peak, calculated using Bragg's law (i.e., $d = 2\pi/q^*$),³⁴ is 5.2 nm. This distance may represent the average spacing between adjacent bilayers in the MLVs.

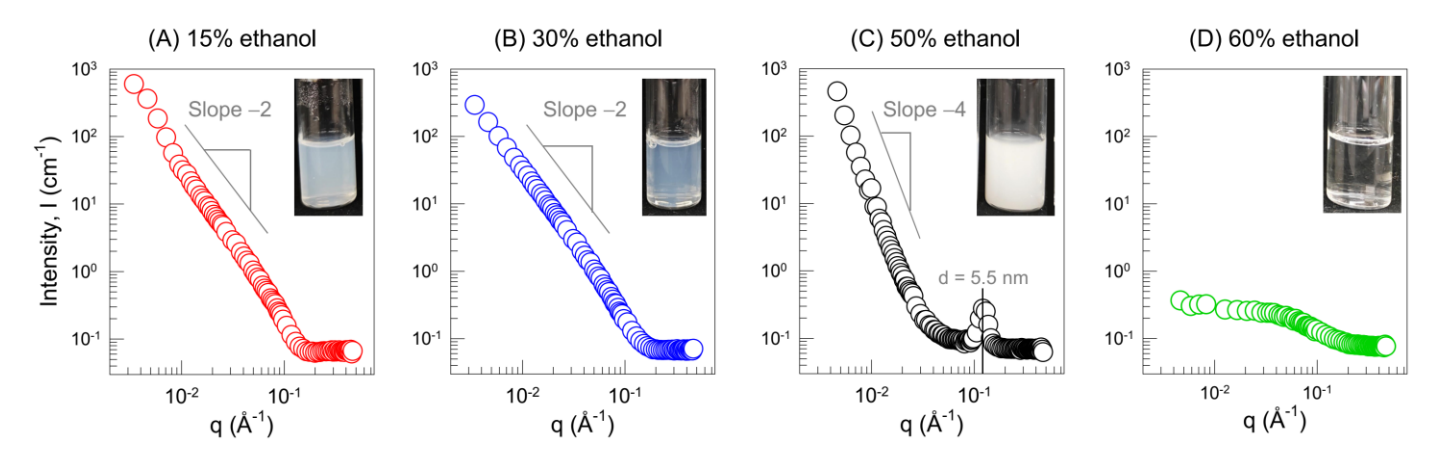


Figure 5. SANS spectra for lecithin samples in deuterated water-ethanol mixtures. Each plot shows the scattered intensity I vs. wave vector q at 25°C. Samples contain 0.5% lecithin. (A) and (B) correspond to vesicles and a slope of -2, reflecting vesicles, is indicated on the plots. (C) The sample is phase-separating, and the presence of interfaces is indicated by Porod scattering (slope of -4). A Bragg peak at high q is also seen. (D) This sample has lower I and a plateau at low Q, reflecting spherical micelles. Vial photos are shown as insets in each plot.

Lastly, SANS data for the sample with 60% ethanol is shown in Figure 5D and it is indicative of small micelles with diameters of a few nm. Spherical or ellipsoidal micelles generally show a I(q) with a plateau at low q and a subsequent decay at higher q, much like the data in Figure 5D.^{29,34} Note also that I at low q is much smaller for this sample compared to the three others — the decreased I implies that much smaller structures are present in this sample. This is again reflective of micelles, which is why the sample is also clear (see inset). Thus, SANS again confirms the previous findings from DLS and cryo-TEM for the nanostructure of lecithin vesicles with increasing f_{eth} : initially there are small vesicles (ULVs), then a transition to larger vesicles (MLVs), then a region of phase-separation, and finally a transition to small micelles.

Lecithin in Water-Methanol and Water-Propanol Mixtures. Given the unusual data for lecithin in water-ethanol mixtures, we wondered if similar results would be observed with other alcohols. Hence, we conducted studies with two other common alcohols: methanol and propanol. OD plots are shown in Figure 6 for 0.5% lecithin in mixtures of water with methanol (Figure 6A), ethanol (Figure 6B, this is a replot from Figure 2), and propanol (Figure 6C). It is interesting to note the similar patterns in all three cases. With increasing alcohol fraction, the

turbidity first decreases, then increases, and finally drops to zero at high alcohol content. Phase-separation and hence a 2-phase region (marked 2ϕ on the plots) is seen with methanol and ethanol: note that this region is larger for ethanol. Note also the different onsets of this 2-phase region: with methanol, it occurs at $f_{\text{meth}} = 73\%$ whereas with ethanol, the onset is at $f_{\text{eth}} = 45\%$. With propanol, there is no 2-phase region; instead, the turbidity increases to a maximum at $f_{\text{prop}} = 18\%$ and then rapidly decays to zero by 22% propanol.

We have found several more interesting features in comparing the various alcohols. First of all, the 2-phase region with methanol is qualitatively different from that with ethanol. In the case of methanol, the sample at 73% methanol separates into two liquid phases, i.e., this is a *liquid-liquid phase separation* (see photos in Figure S7A). In contrast, in the case of ethanol, it is a *solid-liquid phase separation*, i.e., a white precipitate and a clear supernatant (Figure S3). The bottom liquid phase in the 73% methanol sample is slightly viscous and turbid whereas the top liquid phase is clear and non-viscous (Figure S7A). In the case of propanol, the sample at the turbidity maximum ($f_{prop} = 18\%$) is single-phase and shows birefringence under flow (Figure S7B). The birefringence at rest is suggestive of a liquid crystalline phase, possibly

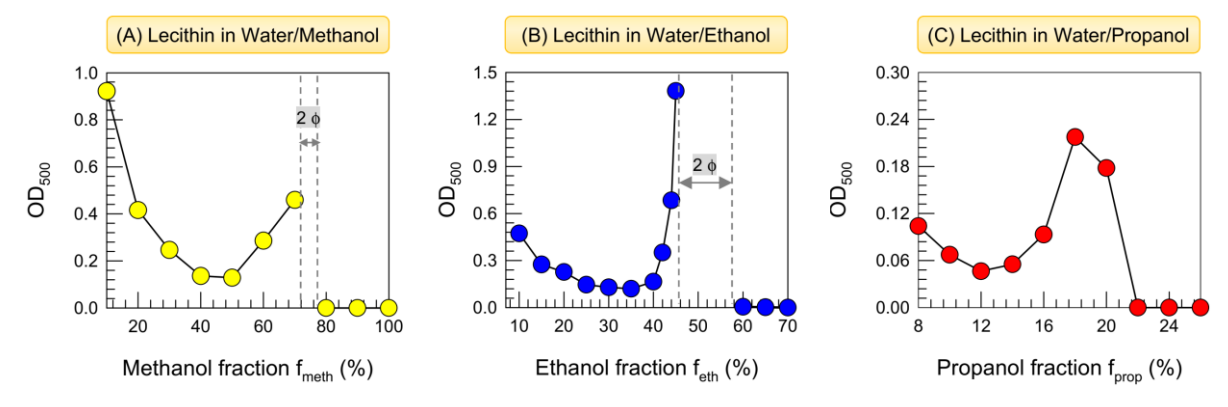


Figure 6. Self-assembly of lecithin in water-alcohol mixtures. Turbidity (OD_{500}) is plotted for 0.5% lecithin vs. the alcohol fraction in the solvent. Data for water-ethanol are reproduced from Figure 2B. Both for methanol (A) and ethanol (B), a 2-phase (2 ϕ) region is seen, and the turbidity rises close to this region. In the case of propanol (C), there is no 2-phase region, but the overall plot has a similar shape.

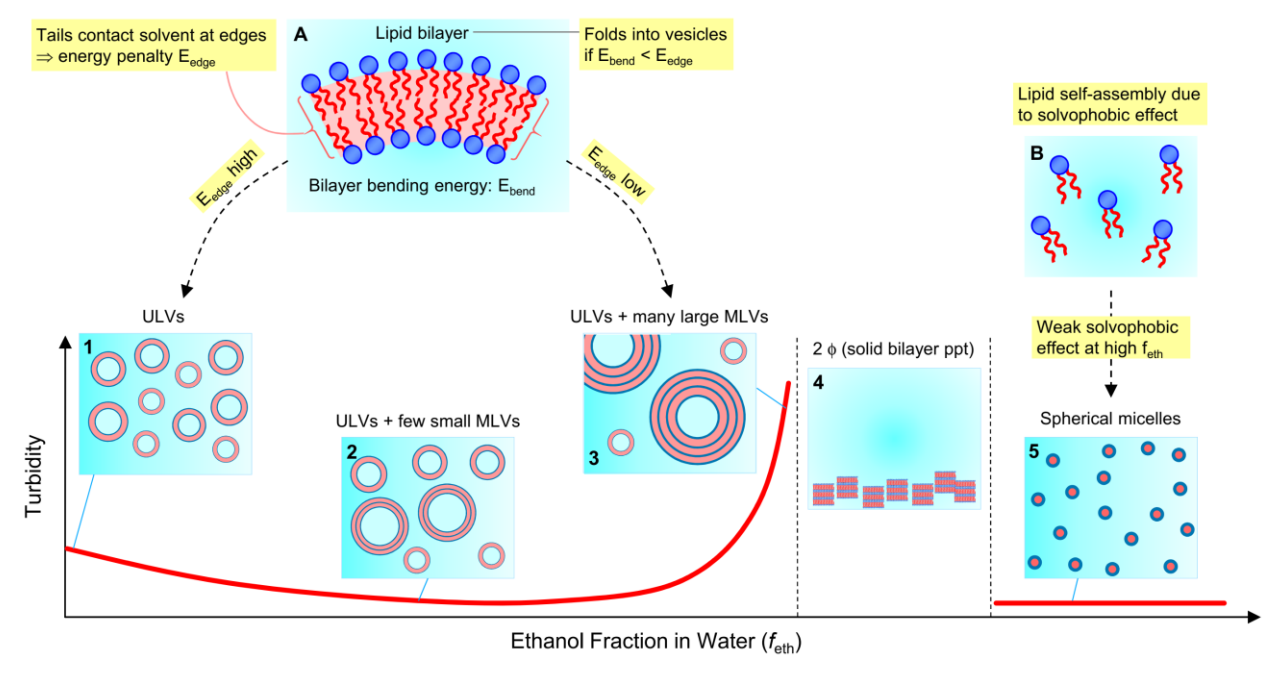


Figure 7. Microstructural changes in lecithin samples as the ethanol fraction is increased. Boxes 1-5 depict the microstructure at different points along a schematic turbidity plot. Boxes 1-3 show a transition from ULVs to MLVs as the 2-phase region is reached. Box A explains why this transition occurs. Box 5 shows a final transition to spherical micelles and Box B explains this.

a lamellar liquid crystal.^{4,5} We should also point out that the region corresponding to spherical micelles (OD \sim 0) has different onsets for the different alcohols: at 80% of methanol, at 60% of ethanol and at 22% of propanol. This follows the order of alcohol polarity,^{4,5} i.e., the least polar alcohol, propanol, is the most effective at solubilizing the lecithin and thereby converting the vesicles into micelles.

Mechanism for Microstructural Changes. To summarize, there are several distinct and unusual features in the turbidity data for lecithin in water-alcohol mixtures. Taking water-ethanol as the prototypical case, we have been able to connect these features to nanostructural changes in the system using DLS, NTA, cryo-TEM and SANS. The key points are:

- Initially, we have ULVs of the lipid.
- For 0-35% ethanol, the vesicles decrease in number.
- At $\sim 35\%$ ethanol, the ULVs grow into large MLVs.
- At $\sim 50\%$ ethanol, the samples become 2-phase.
- At $\sim 60\%$ ethanol, the sample reverts to 1-phase and micelles.

Figure 7 schematically connects all the above microstructural changes with their corresponding changes in turbidity. As the ethanol fraction increases from left to right, Boxes 1-5 show snapshots of the microstructure in the system. When the solvent is mostly water, i.e., $f_{\rm eth} \sim 10\%$, the sample contains vesicles of lecithin that are unilamellar (size ~ 100 nm) and at a high number density $N_{\rm ves}$ (Box 1). When ethanol is increased to $\sim 25\%$, $N_{\rm ves}$ decreases and a few of the vesicles become bilamellar (Box 2), consistent with the cryo-TEM image in Figure 4B. When ethanol is further increased to $\sim 35\%$, we find many large MLVs (> 300 nm) coexisting with smaller ULVs (Box 3), again consistent with the cryo-TEM image in Figure 4C. Additional ethanol ($f_{\rm eth} \sim 50\%$) causes the system to phase separate (Box 4). The solid precipitate coexisting with a clear liquid is likely composed of fused

bilayers. Further addition of ethanol to $\sim 60\%$ results in a phase of small, spherical micelles (~ 5 nm) (Box 5).

Why does the microstructure change as shown in Figure 7? We can break this down into three questions. First, why is there an initial growth from ULVs to MLVs? Thereafter, why a 2-phase region? Finally, why a VMT at higher ethanol? We believe the answers to these questions lie in the dual role played by alcohols on lipid self-assembly, which are highlighted by the two top boxes (A and B) in Figure 7. First it is important to point out that the equilibrium phase formed by selfassembly of lipids is a lamellar phase, i.e., composed of lipid bilayers (sheets).²⁻⁵ When these bilayers bend and fold, they form vesicles.^{2,35,36} The energetic driving force for a bilayer to fold is shown by Box A. At the edge of a bilayer, the lipid tails (shown in red) come into contact with the solvent (light blue). This contact is unfavorable because the tails are hydrophobic. Thus the edges are associated with an energy penalty E_{edge} . When a bilayer folds into a spherical vesicle, the tails are no longer in contact with water, which is why vesicles are favored. However, bending of a bilayer costs energy (E_{bend}) . As long as E_{bend} $< E_{\text{edge}}$, the bilayer will fold into vesicles, and this point is welldescribed in textbooks.2

Now, consider the role of the solvent. $E_{\rm edge}$ will be at its highest when the solvent is pure water. When ethanol is added to water, we expect $E_{\rm edge}$ to drop (Box A). The reason is that lipid tails are soluble in ethanol whereas they are insoluble in water. ^{4,5} Thus, as $f_{\rm eth}$ goes from 0 to 40%, the bilayer edges become more compatible with the solvent. This favors larger vesicles over smaller ones. In other words, bilayer sheets will not need to bend as much in the presence of ethanol and hence will form larger MLVs. This answers the first question as to why ULVs grow into MLVs (Box 1 to 3). The same idea can also address the second question. As MLVs grow too large, they will tend to settle due to gravity instead of remaining in a stable suspension. This is why

we see phase separation at $f_{\rm eth} \sim 50\%$. In the dense bottom phase, the MLVs may also fuse and revert to bilayers, which may account for the solid precipitate in these samples.

Lastly, we discuss the microstructure at $f_{\text{eth}} > 60\%$ by referring to Box B. Why do lipids or surfactants self-assemble into vesicles or micelles? Self-assembly is thermodynamically driven, i.e., by the minimization of the Gibbs free energy. 4,5 The driving force in water is the hydrophobic effect, i.e., it is favorable for hydrophobic tails to be kept away from water in the assembled structure. 4,5 In a solvent other than water, the equivalent is the solvophobic effect, where the tails have a mutual dislike for the solvent. ³⁷⁻³⁹ But the solvophobic effect is much weaker than the hydrophobic effect — this is because water is more polar (and forms stronger hydrogen-bonds) compared to organic solvents.³⁷ For example, taking the dielectric constant ε as a measure of polarity, self-assembly into micelles readily occurs in water (highly polar, $\varepsilon = 80$), and to a weaker extent in glycerol (moderately polar, ε = 47).³⁸ However, self-assembly has not been reported in pure ethanol (weakly polar, $\varepsilon = 25$). Thus, when we increase f_{eth} above 60%, the solvophobic effect will be very weak. In this regime, the only structures that can be formed by self-assembly will be ones with very low aggregation numbers, i.e., small micelles. This explains why a VMT occurs at high ethanol.

Taken together, we emphasize that alcohols exert a dual role on lipid self-assembly, which is observed with, not only ethanol, but also methanol and propanol (Figure 6). At low amounts, alcohols alter the vesicle structure. By reducing the energy penalty at bilayer edges, alcohols induce a transition from ULVs to MLVs. At high amounts, e.g., above 60% in the case of ethanol, the alcohol fraction becomes so high as to reduce the solvophobic effect that drives self-assembly in the first place. In this case, the structures that will be formed in the sample can only be small micelles. Thus, if sufficient alcohol is added to lipid vesicles, it will cause a VMT.

Lecithin in Water-Ethanol: Thermally Induced VMT. In the last section of this paper, we report the interesting response of some lecithin vesicles with varying temperature T. In water-ethanol mixtures (Figure 2), the 2-phase region begins at $f_{\text{eth}} = 45\%$. Samples close to the phase boundary as well as some in the 2-phase region ($f_{eth} = 39$ to 55%) all show a characteristic thermal response. Figure 8 shows data for 0.5% lecithin vesicles at three f_{eth} . These samples are all turbid at low T, but when heated above a temperature T_{VM} , they become clear. The turbidity decrease corresponds to a VMT. The transition temperature $T_{\rm VM}$ decreases as $f_{\rm eth}$ is increased: it is 75°C for 40% ethanol, 60°C for 43% ethanol, and 35°C for 45% ethanol. For $f_{eth} > 45$ %, the samples are 2-phase at room temperature, but these also show a thermal response. As an example, when a sample with 50% ethanol is heated above 28°C, it becomes clear and 1-phase (data not shown). In all cases, the turbidity change at the transition temperature is abrupt, indicating a sharp transition between vesicles and micelles (akin to a phase transition). Also, the VMT is reversible: when a clear sample is cooled below T_{VM}, it reverts to a turbid state. Note also that vesicle samples containing less than 39% ethanol (i.e., sufficiently far away from the phase boundary) do not exhibit any changes in their turbidity with T.

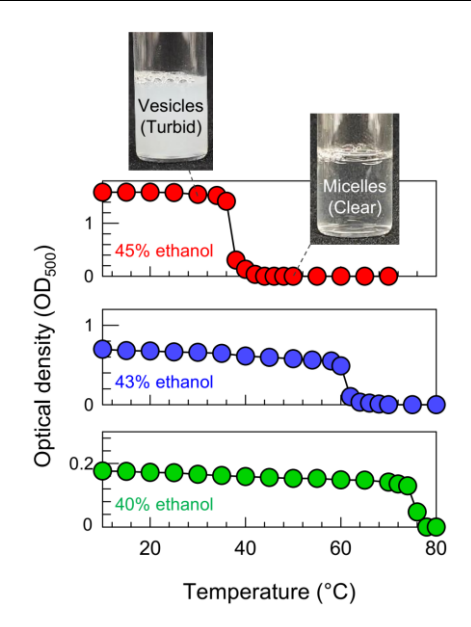


Figure 8 Vesicle-micelle transition upon heating for some lecithin vesicles in water-ethanol mixtures. Samples of 0.5% lecithin at three $f_{\rm eth}$ are studied vs. temperature T and their turbidity (OD₅₀₀) is plotted. In each case, the turbidity sharply drops at a characteristic T, indicating a VMT. Vial photos for the 45% ethanol sample before and after the transition are shown.

SANS confirms that the turbidity changes are associated with a VMT. Spectra for 0.5% lecithin in deuterated water-ethanol at $f_{\rm eth} = 47\%$ are shown in Figure 9. This sample is in the 2-phase region, but it was studied right after preparation when it is homogeneous and turbid. Much like for the sample in Figure 5C, the I(q) plots at low $T(30 \text{ to } 50^{\circ}\text{C})$ in Figure 9A show a slope of -4, reflecting Porod's law $I(I \sim q^{-4})$ for scattering from interfaces. From previous data (Figures 3 and 4), we know that this turbid sample contains large MLVs. When heated further, however, the sample becomes clear, indicating a transition to micelles. Consistent with the visual change, the I(q) plots

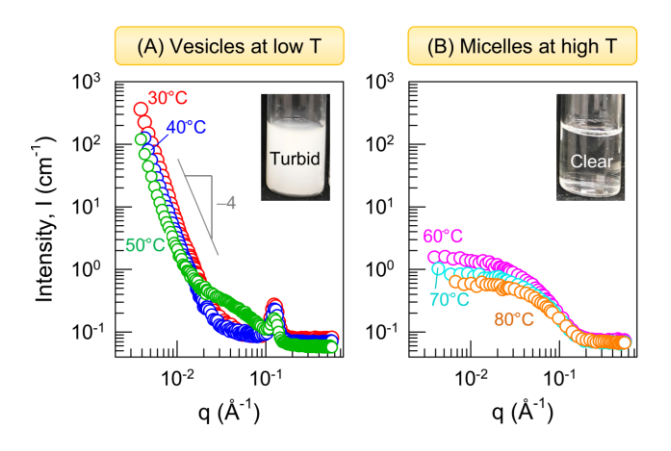


Figure 9. SANS spectra showing a thermally induced VMT. A sample of 0.5% lecithin in deuterated solvents ($f_{\rm eth}$ = 47%) is studied at various T and the scattered intensity I(q) is plotted. (A) At low T, the turbid sample has vesicles and is phase-separating: hence it shows Porod scattering (slope of -4). (B) At high T (above $T_{\rm VM}$), the clear sample has micelles: hence it has lower I and a plateau at low I0. Vial photos are shown as insets.

in Figure 9B at 60 to 80°C show a plateau at low q, characteristic of small micelles (similar to Figure 5D).³⁴ Thus, SANS indeed confirms a thermal VMT in the above sample. Also, previous papers on thermal VMTs in other vesicle systems have reported turbidity and SANS data similar to those in Figures 8 and 9.²⁷⁻³⁰

Why do some lecithin vesicles show a VMT upon heating? One of the previous reports of a thermal VMT in the literature was from our lab in 2006 and the system there was a mixture of a cationic surfactant and an organic acid.²⁹ Equimolar mixtures of the surfactant and the acid formed vesicles, but higher concentrations of the acid caused phase separation. Vesicle samples that were located close to this phase boundary showed a VMT upon heating. Drawing the connection between our previous study and this one, the common pattern is that a thermal VMT occurs for samples close to a phase boundary.²⁹ Indeed, this pattern also extends to other alcohols. For lecithin vesicles in water-methanol (Figure 6A), the phase boundary is at $f_{\text{meth}} = 73\%$. Samples with $f_{\text{meth}} \sim 65$ to 70% show a thermal VMT, as can be noted from the plot in Figure S8A. For lecithin vesicles in water-propanol (Figure 6C), there is no phase boundary, but the turbidity increases to a maxium at $f_{prop} = 18\%$. In this case, samples with $f_{prop} \sim 12-20\%$ show a thermal VMT, and this is evident from the plot in Figure S8B.

Conclusions

We have explored the self-assembly of lecithin in mixtures of water with ethanol and other alcohols. At high volume fractions, alcohols induce lecithin vesicles to undergo a VMT, i.e., convert into micelles, as expected. At lower alcohol fractions, however, we have found an unexpected pattern of microstructural changes and phase behavior. The vesicles (ULVs) initially decrease in number and then grow into larger vesicles with multiple lamellae (MLVs). These MLVs become so large that the system phase-separates. With further alcohol, a single phase is again established, containing micelles. microstructural changes are reflected in the visual appearance of the samples. Lecithin vesicles in water are turbid and when alcohol is added, the turbidity first decreases, then rises sharply until the system phase separates. After a 're-entrant' phase transition (i.e., from 1- to 2and back to 1-phase with increasing alcohol), the samples become clear. Vesicles near the phase boundary moreover show a VMT upon heating. We attribute these findings to the dual role played by alcohols: (a) at low amounts, alcohols reduce the propensity for lipid bilayers to close into spherical vesicles, thereby inducing ULVs to grow into MLVs; (b) at high amounts, alcohols diminish the solvophobic effect, thereby forcing lipid vesicles to convert into micelles. Our findings could be relevant for understanding lecithin self-assembly in biology such as in bile. VMTs induced by alcohol could also be relevant for the delivery of drugs or other solutes in pharmaceuticals, cosmetics, and food science.

Experimental Section

Materials. Lecithin (soy-phosphatidylcholine; 95% purity) was purchased from Avanti Polar Lipids. The solvents methanol, ethanol, and 1-propanol were obtained from Sigma Aldrich. Ultrapure deionized (DI) water from a Millipore filtration system was used to prepare aqueous samples.

Sample Preparation. Vesicles in alcohol-water mixtures were prepared by a simple method, similar to that in our previous studies.³⁹ First, a stock solution of lecithin in a given alcohol was prepared. Then, this solution was mixed with a weighed amount of water corresponding to the desired alcohol:water ratio. The resulting sample was vortex mixed for 120 s. Each sample was equilibrated for at least a day before further analysis. All samples remained stable and unchanged for several days when stored at room temperature.

UV-Vis Spectroscopy. A Varian Cary 50 UV-Vis spectrophotometer was used to measure the optical density (OD), i.e., the absorbance over a 1-cm path length, at a wavelength of 500 nm. The OD is a measure of sample turbidity. For the OD measurements as a function of temperature, a Peltier-controlled cell, connected to a water bath, was used to maintain the temperature.

Dynamic Light Scattering (DLS). Vesicle sizes were measured at 25°C using a Photocor-FC instrument equipped with a 5 mW laser source at 633 nm, with the scattering angle being 90°. The autocorrelation function was measured using a logarithmic correlator and analyzed by the DynaLS software package to obtain the distribution of hydrodynamic diameters and thereby the average diameter.

Small Angle Neutron Scattering (SANS). SANS experiments were performed at the NIST Center for Neutron Research (NCNR), Gaithersburg, MD on the NG-B (30 m) beamline. Neutrons with a wavelength λ of 6 Å were selected and the range of wave-vectors q accessed was from 0.004 to 0.4 Å⁻¹. The sample holders were 1 mm titanium cells with quartz windows. The scattering data was reduced using IGOR-Pro software and were corrected to obtain an absolute scale of scattering intensity using NIST calibration standards.

Cryogenic Transmission Electron Microscopy (Cryo-TEM). A small drop (3.5 μ L) of a given sample was pipetted onto a C-flat holey carbon grid (Protochips) and excess liquid was blotted off using filter paper. The grid was then plunged into liquid ethane at a temperature of -173°C using a Cryoplunger 3 system (Gatan). The vitrified thin specimen was then transferred to a cryo-TEM holder (Gatan 652) using a cryo-workstation and then transferred to the microscope, where a temperature of -176°C was maintained using liquid nitrogen. A JEOL 2100 LaB6 TEM at an accelerating voltage of 100 kV was used to image the sample.

Nanoparticle Tracking Analysis (NTA). Vesicle concentrations were measured using a ZetaView® BASIC NTA Microscope (Particle Metrix). Samples were diluted such that the measured concentrations were around 10⁷ particles/mL (~200 particles per frame). Concentrations were measured by scanning 11 cell positions at 30 frames per position over 2 cycles. The sensitivity for video acquisition was set to 80, and the shutter speed to 100.

Acknowledgements: We acknowledge funding from NSF CBET #2226547 to SRR and through a Wylie Fellowship to FAB. We thank Dr. Wen-An Chiou from the NISP lab for assistance with the cryo-TEM experiments; Prof. Hannah Zierden for allowing us the use of the NTA in her lab; Prof. Taylor Woehl for allowing us the use of the spectrometer in his lab; and the NCNR for enabling the SANS

experiments performed as part of this work. We thank Dr. Norman Javitt from the Department of Medicine at New York University (NYU) for stimulating discussions regarding vesicles in bile. We also thank Medha Rath, Kerry DeMella, Sohyun Ahn, and Ben Thompson for their assistance with various experiments.

Supporting Information: Additional experimental results (pdf). Number of pages: 5; number of figures: 8.

References:

- [1] Luisi, P. L. The Emergence of Life: From Chemical Origins to Synthetic Biology; Cambridge University Press: Cambridge, 2016.
- [2] Boal, D. *Mechanics of the Cell*; Cambridge University Press: Cambridge, 2002.
- [3] Phillips, R.; Kondev, J.; Theriot, J.; Garcia, H. *Physical Biology of the Cell*; CRC Press, 2012.
- [4] Evans, D. F.; Wennerstrom, H. The Colloidal Domain: Where Physics, Chemistry, Biology, and Technology Meet; Wiley-VCH: New York, 2001.
- [5] Israelachvili, J. N. Intermolecular and Surface Forces; Academic Press: San Diego, 2011.
- [6] Lecithins and Phospholipids: Biochemistry, Properties and Clinical Significance; Hernandez, J., Ed.; Nova Science Publishers, 2015.
- [7] Reshetnyak, V. I. "Physiological and molecular biochemical mechanisms of bile formation." World J. Gastroenterol. 2013, 19, 7341-7360.
- [8] Crawford, J. M.; Mockel, G. M.; Crawford, A. R.; Hagen, S. J.; Hatch, V. C.; Barnes, S.; Godleski, J. J.; Carey, M. C. "Imaging biliary lipid secretion in the rat - ultrastructural evidence for vesiculation of the hepatocyte canalicular membrane." *J. Lipid Res.* 1995, 36, 2147-2163.
- [9] Wang, A. N.; Miller, C. C.; Szostak, J. W. "Core-shell modeling of light scattering by vesicles: Effect of size, contents, and lamellarity." *Biophys. J.* 2019, 116, 659-669.
- [10] Lichtenberg, D.; Robson, R. J.; Dennis, E. A. "Solubilization of phospholipids by detergents - structural and kinetic aspects." *Biochim. Biophys. Acta* 1983, 737, 285-304.
- [11] De la Maza, A.; Parra, J. L. "Vesicle-micelle structural transition of phosphatidylcholine bilayers and Triton X-100." *Biochem. J.* 1994, 303, 907-914.
- [12] Ahyayauch, H.; Larijani, B.; Alonso, A.; Goñi, F. M. "Detergent solubilization of phosphatidylcholine bilayers in the fluid state: Influence of the acyl chain structure." *Biochim. Biophys. Acta* 2006, 1758, 190-196.
- [13] Tsengam, I. K. M.; Omarova, M.; Kelley, E. G.; McCormick, A.; Bothun, G. D.; Raghavan, S. R.; John, V. T. "Transformation of lipid vesicles into micelles by adding nonionic surfactants: Elucidating the structural pathway and the

- intermediate structures." J. Phys. Chem. B 2022, 126, 2208-2216.
- [14] Long, M. A.; Kaler, E. W.; Lee, S. P. "Structural characterization of the micelle-vesicle transition in lecithin-bile salt-solutions." *Biophys. J.* 1994, 67, 1733-1742.
- [15] Elsayed, M. M. A.; Cevc, G. "The vesicle-to-micelle transformation of phospholipid-cholate mixed aggregates: A state of the art analysis including membrane curvature effects." *Biochim. Biophys. Acta-Biomembr.* 2011, 1808, 140-153.
- [16] Kiselev, M. A.; Janich, M.; Hildebrand, A.; Strunz, P.; Neubert, R. H. H.; Lombardo, D. "Structural transition in aqueous lipid/bile salt [DPPC/NaDC] supramolecular aggregates: SANS and DLS study." *Chem. Phys.* 2013, 424, 93-99.
- [17] Haustein, M.; Wahab, M.; Mögel, H. J.; Schiller, P. "Vesicle solubilization by bile salts: Comparison of macroscopic theory and simulation." *Langmuir* 2015, 31, 4078-4086.
- [18] Cohen, D. E.; Angelico, M.; Carey, M. C. "Structural alterations in lecithin-cholesterol vesicles following interactions with monomeric and micellar bile-salts - physical-chemical basis for subselection of biliary lecithin species and aggregative states of biliary lipids during bile formation." *J. Lipid Res.* 1990, 31, 55-70.
- [19] Soderberg, I. "Phase-behavior and structure in the soybean phosphatidylcholine-ethanol-water system." *Progr. Colloid Polym. Sci.* 1989, 82, 285-289.
- [20] Aarts, P.; Gijzeman, O. L. J.; Kremer, J. M. H.; Wiersema, P. H. "Dynamics of phospholipid aggregation in ethanol-water solutions." *Chem. Phys. Lipids* 1977, 19, 267-274.
- [21] Taraschi, T. F.; Rubin, E. "Effects of ethanol on the chemical and structural-properties of biologic membranes." *Lab. Invest.* 1985, 52, 120-131.
- [22] Goldstein, D. B. "Effect of alcohol on cellular membranes." Ann. Emerg. Med. 1986, 15, 1013-1018.
- [23] Zysset, T.; Polokoff, M. A.; Simon, F. R. "Effect of chronic ethanol administration on enzyme and lipid properties of liver plasma-membranes in long and short sleep mice." *Hepatology* 1985, 5, 531-537.
- [24] Richard, C.; Cassel, S.; Blanzat, M. "Vesicular systems for dermal and transdermal drug delivery." RSC Adv. 2021, 11, 442-451.
- [25] Touitou, E.; Dayan, N.; Bergelson, L.; Godin, B.; Eliaz, M. "Ethosomes - novel vesicular carriers for enhanced delivery: characterization and skin penetration properties." *J. Control. Release* 2000, 65, 403-418.
- [26] Ogunsola, O. A.; Kraeling, M. E.; Zhong, S.; Pochan, D. J.; Bronaugh, R. L.; Raghavan, S. R. "Structural analysis of "flexible" liposome formulations: new insights into the skinpenetrating ability of soft nanostructures." *Soft Matter* 2012, 8, 10226-10232.
- [27] Hassan, P. A.; Valaulikar, B. S.; Manohar, C.; Kern, F.; Bourdieu, L.; Candau, S. J. "Vesicle to micelle transition: Rheological investigations." *Langmuir* **1996**, *12*, 4350-4357.

- [28] Buwalda, R. T.; Stuart, M. C. A.; Engberts, J. "Wormlike micellar and vesicular phases in aqueous solutions of singletailed surfactants with aromatic counterions." *Langmuir* 2000, 16, 6780-6786.
- [29] Davies, T. S.; Ketner, A. M.; Raghavan, S. R. "Self-assembly of surfactant vesicles that transform into viscoelastic wormlike micelles upon heating." *J. Am. Chem. Soc.* 2006, 128, 6669-6675.
- [30] McCoy, T. M.; Marlow, J. B.; Armstrong, A. J.; Clulow, A. J.; Garvey, C. J.; Manohar, M.; Darwish, T. A.; Boyd, B.; Routh, A. F.; Tabor, R. F. "Spontaneous self-assembly of thermoresponsive vesicles using zwitterionic and an anionic surfactant." *Biomacromolecules* 2020, 21, 4569-4576.
- [31] Liu, J. N.; Harms, M.; Garamus, V. M.; Müller-Goymann, C. C. "Reentrant structural phase transition in amphiphilic selfassembly." Soft Matter 2013, 9, 6371-6375.
- [32] Portz, B.; Shorter, J. "Biochemical timekeeping via reentrant phase transitions." *J. Mol. Biol.* **2021**, *433*, 166794.
- [33] Filipe, V.; Hawe, A.; Jiskoot, W. "Critical evaluation of Nanoparticle Tracking Analysis (NTA) by NanoSight for the measurement of nanoparticles and protein aggregates." *Pharm. Res.* 2010, 27, 796-810.
- [34] Pedersen, J. S. "Analysis of small-angle scattering data from colloids and polymer solutions: modeling and least-squares fitting." *Adv. Colloid Interface Sci.* **1997**, *70*, 171-210.
- [35] Lasic, D. D. "The mechanism of vesicle formation." *Biochem. J.* 1988, 256, 1-11.
- [36] Sackmann, E. "Membrane bending energy concept of vesicle-shape and cell-shape and shape-transitions." FEBS Lett. 1994, 346, 3-16.
- [37] Moya, M. L.; Rodriguez, A.; Graciani, M. D.; Fernandez, G. "Role of the solvophobic effect on micellization." *J. Colloid Interface Sci.* **2007**, *316*, 787-795.
- [38] Agrawal, N. R.; Yue, X.; Feng, Y. J.; Raghavan, S. R. "Wormlike micelles of a cationic surfactant in polar organic solvents: Extending surfactant self-assembly to new systems and subzero temperatures." *Langmuir* **2019**, *35*, 12782-12791.
- [39] Agrawal, N. R.; Omarova, M.; Burni, F.; John, V. T.; Raghavan, S. R. "Spontaneous formation of stable vesicles and vesicle gels in polar organic solvents." *Langmuir* 2021, 37, 7955-7965.

TOC Graphic

